Monitoring a Person's Heart Rate and Respiratory Rate on a Shared Bed Using Geophones

Zhenhua Jia †, Amelie Bonde §, Sugang Li †, Chenren Xu ‡, Jingxian Wang §, Yanyong Zhang †, Richard E. Howard †, Pei Zhang §

† Wireless Information Network Laboratory, Rutgers University
§ Department of Electrical and Computer Engineering, Carnegie Mellon University
‡ Center for Energy-efficient Computing and Applications, Peking University

ABSTRACT

Using geophones to sense bed vibrations caused by ballistic force has shown great potential in monitoring a person's heart rate during sleep. It does not require a special mattress or sheets, and the user is free to move around and change position during sleep. Earlier work has studied how to process the geophone signal to detect heartbeats when a single subject occupies the entire bed. In this study, we develop a system called VitalMon, aiming to monitor a person's respiratory rate as well as heart rate, even when she is sharing a bed with another person. In such situations, the vibrations from both persons are mixed together. VitalMon first separates the two heartbeat signals, and then distinguishes the respiration signal from the heartbeat signal for each person. Our heartbeat separation algorithm relies on the spatial difference between two signal sources with respect to each vibration sensor, and our respiration extraction algorithm deciphers the breathing rate embedded in amplitude fluctuation of the heartbeat signal.

We have developed a prototype bed to evaluate the proposed algorithms. A total of 86 subjects participated in our study, and we collected 5084 geophone samples, totaling 56 hours of data. We show that our technique is accurate – its breathing rate estimation error for a single person is 0.38 breaths per minute (median error is 0.22 breaths per minute), heart rate estimation error when two persons share a bed is 1.90 beats per minute (median error is 0.72 beats per minute), and breathing rate estimation error when two persons share a bed is 2.62 breaths per minute (median error is 1.95 breaths per minute). By varying sleeping posture and mattress type, we show that our system can work in many different scenarios.

CCS CONCEPTS

•**Human-centered computing** →**Ubiquitous and mobile computing systems and tools;**

KEYWORDS

Vital Signs, Geophone, Unobtrusive Sensing, Blind Source Separation, Time-frequency Masking

1 INTRODUCTION

Monitoring a person's vital signs during sleep, especially heart rate and respiratory rate, has received a great deal of attention in the last few years. Many systems [2, 3, 10, 18, 21, 22, 25, 27, 30, 32, 40, 49, 51, 52, 54] have been proposed in both industry and academia, promising to potentially serve as a proxy to various health/medical applications, such as monitoring sleep quality [53], detecting obstructive sleep apnea [38], evaluating the risk of heart failure under certain situations [29, 39], and even monitoring patients with Parkinson's diseases [12], etc.

Most of these systems monitor vital signs by measuring one or more aspects of the ballistic force during a heartbeat pulse, ranging from force magnitude [18, 40], pressure [25, 49], to the resulting position change [10, 21, 32, 51, 52, 54]. Even though they are able to perform accurate monitoring, most of them are quite cumbersome to install on a bed (e.g., requiring special mattress/sheets, requiring the user to keep the same sleeping position/posture, etc), or are inconvenient/invasive to the users.

Recent work [27] has shown that the geophone sensor [4], which measures the vibration velocity caused by ballistic force, provides a viable alternative in detecting heart rate during sleep without having the above problems of the existing systems. Thanks to being sensitive to even minute vibrations, geophones offer accurate monitoring, are easy to install, can be installed anywhere on the bed frame, and do not assume any sleeping patterns from the user.

Despite these nice features, a great deal of effort is still required to build a full-fledged vital sign monitoring system using the geophone sensor. First, we need to detect respiration using geophones, which is very difficult because the vibrations caused by respiration are weak and the frequency components are below the extremely low frequency (ELF) band (<1 Hz). Thus geophones don't capture those vibrations well. Second, we need to extract the target subject's heart rate from the mixed vibration signal when multiple people share a bed. The difficulty of this problem is mainly due to the fact that the heartbeat vibration signals are mixed together in the time domain and the frequency components from multiple people can be quite close to each other. In this paper, we seek to develop *VitalMon*,
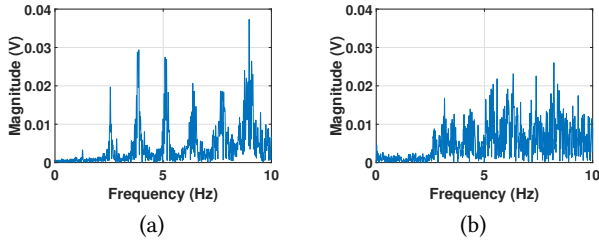
Figure 1: (a) The geophone signal in the frequency domain, with a single subject on the bed, and (b) the geophone signal in the frequency domain, with two subjects on the bed. Peaks caused by heartbeats and harmonics are obvious in (a), making single-subject heart rate monitoring rather simple. When we have two subjects on one bed, however, heartbeat peaks are less obvious and hard to detect directly.

an in-bed heart rate and respiratory rate monitoring system using geophones, and set out to address these two challenges.

Challenges of Respiration Monitoring: Detecting respiration using geophones is challenging. A geophone is naturally a velocity sensor and a second-order high-pass filter, thus insensitive to low-speed low-frequency vibrations. Unfortunately, the vibration speed of the thoracic cavity during each breath is slow compared to the ballistic movement of a heartbeat, and the respiration signal frequency is low.

In general, the vibration signal caused by each respiration event is so weak that the respiration signal is buried under noise from the environment. In this paper, we propose an alternative approach by modeling the geophone signal as a signal after amplitude modulation (AM). Here, the heartbeat signal is our carrier signal and the respiration signal is our information signal. Then, we use a square-law amplitude demodulation (SLD) algorithm [9] combined with autocorrelation function (ACF) [15] to estimate the respiratory rate.

Challenges of Heart Rate Monitoring: Even though earlier work [27] has shown that geophones are suitable to monitor heart rate when the person occupies a bed alone, monitoring a person's heart rate when he/she shares the bed with others remains an unsolved challenge. The heartbeat vibration signals from the bed occupants are mixed together in the time domain during propagation, and the frequency of the heartbeat signals and respiration signals from multiple people can be very close in the frequency domain. Figures 1 (a) and (b) show two Fast Fourier Transform (FFT) examples of the vibration signals when we have (a) one person on a bed, with a heart rate of 76.7 BPM_{hr}[1] (about 1.28 Hz), and (b) two people on one bed, with heart rates of 62.8 (about 1.05 Hz) and 59.2 BPM_{hr} (about 0.99 Hz), respectively. It is hard to tell there are two heartbeats from the mixed signal. In fact, the amplitude at different frequencies is even smaller than when we had only one subject, mainly due to the relative phase delay between two heartbeat signals. Furthermore, heartbeats over time are not perfectly periodic. Therefore, it is hard to separate them in both time and frequency

domains. In this study, we address this challenge by taking advantage of the spatial differences between two heartbeats. Suppose we have two geophones G_1 and G_2. As far as the source closer to G_1 is concerned, its vibration signal captured by G_1 has higher amplitude and less phase delay compared to the same source's signal captured by geophone G_2. Based upon this spatial difference, we can extract the target source's signal from the mixture.

Considering the similarity between heartbeat signals and human sound signals, and how they are similarly mixed together in real life, we turn to literature in the acoustic field for wisdom. Popular solutions include Independent Component Analysis (ICA) [26], Principal Component Analysis (PCA) [28], etc. Among the solutions that have been proposed, Degenerate Unmixing Estimation Technique (DUET) [48, 55] is well-suited to address our needs because (1) unlike ICA, it can tolerate propagation delays; and (2) the sudden change in a heartbeat signal may make consecutive heartbeat pulses look uncorrelated, which may trick some methods into treating those signals as independent, but has less impact on the DUET because it does not rely solely on such correlation.

Applying DUET to our heartbeat separation problem is not straightforward, due to the unique characteristics of heartbeat signals that propagate through a bed. Firstly, the fundamental frequency of a heartbeat is significantly lower than that of the audio signal. Its average range is from 0.33 Hz to 4 Hz, corresponding to 20 BPM_{hr} (e.g., the heart rate for patients with heart block disease) to 240 BPM_{hr} (the maximum heartbeat rate estimated based on the minimum cardiac refractory period of a human being), respectively. As a result, we need high frequency resolution when we extract individual heartbeats from a mixture, which is particularly challenging for us because heartbeats are not perfectly periodic and stable.

Secondly, the bed and mattress have much more complex propagation properties than air. The grouping velocity of any vibration through a bed is around 1 km/s, whose form is a complex mechanical resonance depending on the details of the entire system – e.g., the human body, the bed, the geophone, and the floor, etc.

In addition, the structure of a modern bed often allows vibrations to last for at least a few cycles, and for a heartbeat signal, the preceding heartbeat may affect the subsequent ones. Because of these complex propagation properties, each heartbeat source's spatial signatures become less separable than audio signals, making heartbeat separation a much harder problem.

Our Contributions: In this study, we carefully design the VitalMon system to solve these challenges. For heart rate estimation, we take advantage of the high frequency components of the heartbeat signals, such as the harmonics, so that we have larger frequency differences between different heartbeat signals to enable smaller window sizes. For respiratory rate estimation, we model the signal as AM and use the modulated signal itself to achieve demodulation, which allows us to apply demodulation without knowing the frequency of the carrier signal (heartbeats in our case). Through detailed experimentation, we show that VitalMon can successfully monitor the target person's respiration and heart rate, even when he/she shares the bed with others. We measured a total of 5084 data sets and collected vital sign signals over 56 hours[2]. The overall

---

[1]In this paper, we use BPM_{hr} to denote 'beats per minutes' for heart rate and BPM_{rr} to denote 'breaths per minute' for respiratory rate.

[2]Our studies were approved by the Institutional Review Board (IRB) of our institution.

absolute estimation error for heart rate and respiratory rate is at 1.90 BPM_{hr} and 2.62 BPM_{rr}, respectively, and the median is 0.72 BPM_{hr} and 1.95 BPM_{rr}.

In summary, our work has made the following contributions:

(1) We have developed a respiration detection technique based on square-law amplitude demodulation that can estimate the respiratory rate from the vibration signals. To our best knowledge, this is the first paper which shows that the overall amplitude of a heartbeat signal is modulated to carry the respiration signal and we show our technique can successfully demodulate the respiratory rate information.

(2) We have developed a heartbeat separation technique that can accurately track the heartbeat of a specific person when there are multiple people on one bed. In developing our technique, we have taken into consideration the unique properties of heartbeat signals as well as the complex propagation properties of the bed and mattress.

(3) We have developed a testbed with multiple vibration sensors (geophones in our case). In developing the testbed, we have taken into consideration the features of geophone sensors and their placement.

2 BACKGROUND AND OVERVIEW

In this section, we first provide the background on ballistocardiograph (BCG) based heart rate and respiratory rate monitoring. Then we present an overview of our geophone-based BCG measurement system.

2.1 BCG Based Heart Rate and Respiratory Rate Monitoring

Many BCG based systems have been developed to monitor a person's physiological signs by sensing the ballistic force on the heart. The earliest work we can find was done by J. W. Gordon in 1877 [23]. He designed an analog BCG system which consists of (1) a special designed mattress that is small but stiff, (2) four ropes to hang the mattress to the ceiling in a room, (3) a bunch of levers to amplify the analog vibration signal, and (4) a weighing machine to record the signal on paper. Despite of the cumbersome nature of such a system, it successfully captured the weak vibrations from each heartbeat. Later, many BCG-based systems have been proposed and we categorize them below based on the sensor types:

(1) Force sensors [18, 40], commonly installed under bed posts, measure the force change due to the ballistic force. The idea is straightforward, but it requires a fairly high sensitivity since it tries to detect a weak force change under the influence of the gravity of the bed and people.

(2) Air/water pressure sensors [25, 34, 49], usually sandwiched between mattress and bed frame, measure the pressure exerted by the ballistic force. Due to the limitation of the sensitivity, the sensor should be installed under the thorax area of the human body, which requires prior knowledge of the person's location on the bed.

(3) Position sensors measure the position change due to the ballistic force. Position change can be detected by a variety of means. For example, an optical sensor can detect position change when it is embedded in a mattress and placed in the thorax area [51, 52]; an ultrasound-based sensor can detect position change [54], but requires mounting a plywood board and an aluminum guide rail on the bed frame; a wireless-based system can also detect position change [10], but requires additional wireless infrastructure and could be easily interfered by other wireless signals in the environment.

(4) Accelerometer sensors can detect the vibration acceleration caused by the ballistic force, such as a chest belt [45] or the commercial system in [5]. However, such a system is invasive and uncomfortable.

(5) Velocity sensors, such as geophones [27], measure the speed of vibrations caused by the ballistic force. They can be attached anywhere on a bed, and are unobtrusive and convenient.

2.2 VitalMon Overview

Among the above BCG monitoring systems, the velocity sensing approach offers accurate, unobtrusive, low-cost, and robust monitoring, as shown in a recent study [27]. In this study, we use a commercial off-the-shelf geophone, which is a moving coil based velocity sensor.

Geophones, traditionally used to measure seismic waves in geology, have been widely used in measuring vibrations from different sources. Recently, geophones have been used in several applications: building occupancy estimation by monitoring ambient vibration [41], indoor person localization via floor vibration [36], interaction tracking via surface vibration [42], heart rate estimation by monitoring bed vibration during sleep [27], etc. A geophone consists of a spring-mounted magnetic mass moving within a coil. It converts the physical vibration from the environment into an electrical voltage. The geophone we use, SM-24 Geophone Elements [4], is naturally a second-order high-pass filter and its natural frequency is 10 Hz.

The overview of VitalMon is illustrated in Figure 2. In VitalMon, our objective is to *continuously monitor the heart rate and breathing rate of our user (say, Alice), whether Alice occupies a bed alone or shares a bed with Bob.* For monitoring purposes, we use the same number of geophones as the number of persons on a bed. When both Alice and Bob are present, we use two geophones to measure the vibrations caused by their heartbeats and breathing. Since heartbeats lead to much more pronounced vibrations than breathing, we first extract Alice's heartbeat signals (the amplitude and frequency) from the geophone signals. Then we further extract the respiration signal from her heartbeat signals. Both steps introduce serious challenges, and we have devised efficient techniques to address them. In the following two sections, we present our proposed signal processing techniques – we first focus on how to extract respiration from heartbeat signals, and then focus on how to extract individual heartbeat signals from the mixture signal.

3 MONITORING RESPIRATORY RATE USING GEOPHONE

In this section, we discuss how we monitor the respiratory rate using geophones, assuming there is only one person on a bed.
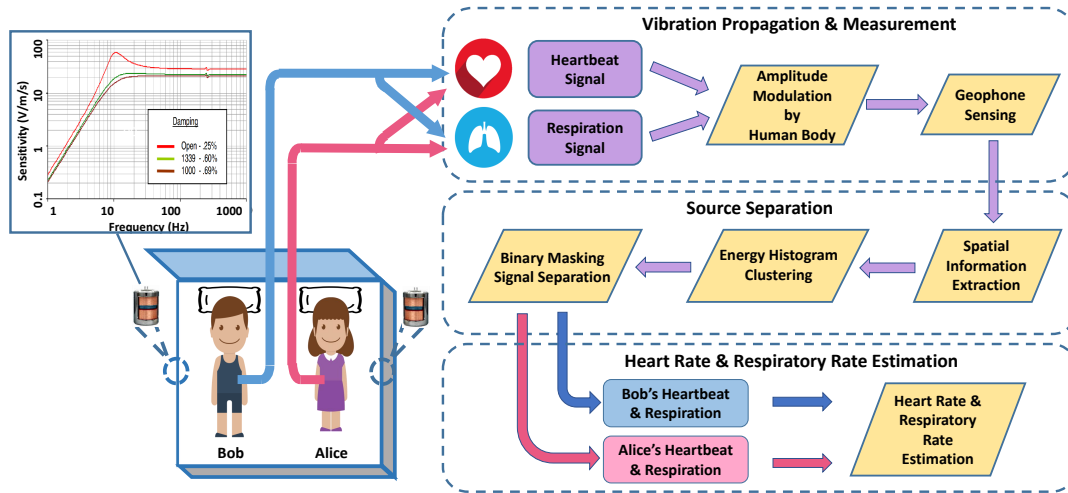
Figure 2: The overview of VitalMon. When two persons (Alice and Bob) share a bed, we use two geophones to capture the mixed vibration signals, and then perform a sequence of signal processing steps to monitor the heart rate and breathing rate of our target user (say, Alice).
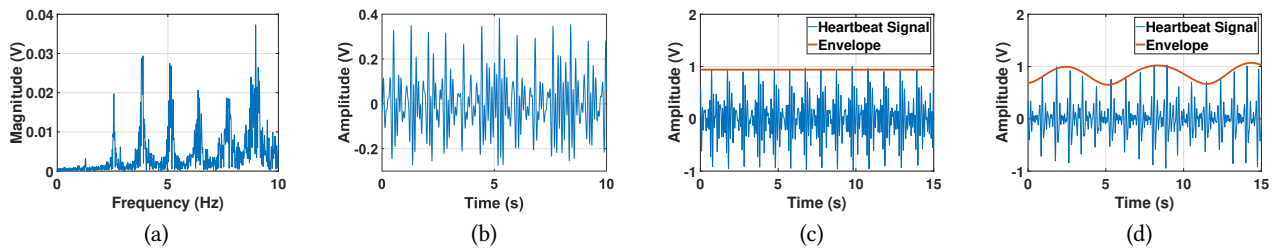

Figure 3: (a) The geophone signal in the frequency domain, with a single person on the bed, (b) the same geophone signal as in (a), but in the time domain, (c) the geophone signal with a single person holding his breath, and (d) the geophone signal with a single person breathing normally. In (b) and (d), the subject's breathing rate is embedded in the heartbeat signal amplitude fluctuation, or the envelope.

We first formulate the respiration signal extraction problem as an amplitude modulation problem. We then explain the difference between our problem and the traditional amplitude problem in communications. Finally, we present our amplitude demodulation algorithm.

3.1 Formulating Respiration Signals as Amplitude Modulation

The most straightforward approach to extracting the respiration signal would involve directly performing FFT on the geophone signal and then looking for the frequency component corresponding to respiration. However, as shown in Figure 3 (a), we don't observe any obvious respiration frequency components (that should be below 1 Hz) from the geophone signal. This is because a geophone is a natural second-order high-pass filter, insensitive to motions whose frequencies are below a certain threshold (referred to as detection threshold, 8.4 Hz in our case). The frequency components of respiration are usually lower than this detection threshold. Also, the velocity of breathing is quite slow, which makes it even harder to detect by geophones. As a result, this direct approach fails to detect respiration signals.

On the other hand, a closer look at the geophone signal reveals an interesting phenomenon – the amplitude of the geophone signal fluctuates in a periodic fashion, and the fluctuation frequency is very close to the subject's breathing frequency. For example, in Figure 3(b), the subject's respiratory rate is 15.04 BPM_{rr}, which is very close to the amplitude fluctuation frequency of 0.251 Hz. To further investigate this observation, we conducted an experiment and compared the geophone signals when the subject held his breath with the signals when the subject breathed normally. Figure 3(c) shows the geophone signal when a subject lies on a bed while holding his breath for at least 15 seconds, while Figure 3(d) shows the geophone signal when the subject breathes at a rate of 10 BPM_{rr}. In both figures, we plot the estimated envelope of the signals. It is clear that there is a direct relationship between breathing and the amplitude fluctuation.

After deliberation, we conclude that respiration causes the amplitude fluctuation of the geophone signal. It can be explained as follows. Breathing changes the amount of air in the chest, which in turn changes the effective 'stiffness' of the chest and the amount of energy loss of the heartbeat signal after propagation through the chest. As such, the relationship between the respiration signal and the heartbeat signal can be modeled as amplitude modulation

(AM) in communications [46]. Here, the heartbeat signal, including its fundamental frequency and the associated harmonics, is the carrier signal, the respiration signal is the information signal, and the geophone signal is the signal after amplitude modulation.

Following amplitude modulation, we can model the three signals as follows:

$$
\begin{aligned}
s(t) &= s_r(t) \sum_{j=1}^{N} s_{h_j}(t), \\
s_r(t) &= a_r \times cos(2\pi f_r t + \theta_i), \\
s_{h_j}(t) &= a_{h_j} \times cos(2\pi f_{h_j} t + \theta_{h_j}), j = 1, 2, ..., N,
\end{aligned}
\tag{1}
$$

where $s(t)$ denotes the source signal for single person case, s_r denotes the respiration signal and s_{h_j} denotes the j-th harmonics of the heartbeat signal. Note, s_{h_1} means the fundamental frequency of the heartbeat signal.

Next, we devise a suitable amplitude demodulation algorithm to extract the respiratory rate information from the geophone signal. However, our problem significantly differs from the conventional RF amplitude modulation problem in that the RF signal's carrier frequencies are known beforehand, while the frequency of our carrier signal – the heartbeat signal – remains unknown. To make matters worse, unlike the RF signal which has a single carrier frequency, the heartbeat signal includes a fundamental frequency and multiple higher frequency components.

Due to these differences, typical detectors for demodulating AM signals that were proposed for RF signals are ill suited for our problem. For example, an envelope detector, such as the Moving Root-Mean-Square (RMS) envelopes approach [43] or the analytic signal approach [31], is sensitive to the choice of the window size; window size depends on the frequency of the information signal, which is unknown in our case. The RMS envelopes approach also doesn't work well with an impulse-like signal such as the ballistic force within each heartbeat. Meanwhile, a product detector [44] usually requires knowledge of the carrier frequency, which is again unknown in our case. Finally, neither of these detectors work well when carrier signals are quasi-periodic, like heartbeats in our system.

Therefore, we choose the square-law demodulation approach in this study, using the geophone signal as the carrier signal which can demodulate itself to extract the information signal (the respiration signal in our case). AM during propagation shifts the respiration frequency components to a higher frequency range (around the heartbeat frequency range). By squaring the signal, we reverse the frequency shift and can separate the respiration signal by applying a low-pass filter.

3.2 Respiratory Rate Estimation

Next, we present our respiratory rate estimation algorithm based on the square-law demodulation.

Before presenting our algorithm, we first discuss how we estimate the environmental noise and eliminate its impact. We do so by recording the geophone signal when the bed is empty and computing the FFT. The FFT results show that the majority of the noise is above 11 Hz. We note that our lab environment has a considerably greater noise level than an average bedroom environment as we have a few hundred computers sharing the same lab space,
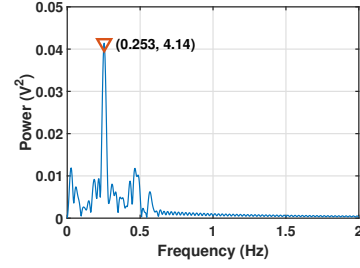

Figure 4: FFT of the power signal after our amplitude demodulation. We observe a peak at 0.253 Hz (marked with a red inverted triangle), which corresponds to a respiratory rate of 15.18 BPM_{rr} and agrees with the ground truth measured by a Zephyr strip [8].

most of which are equipped with powerful fans. Next, we collect the geophone signal when a single subject is lying on a bed. The corresponding FFT results show the frequency components of our target signals (heartbeat signals and respiration signals) are below 15 Hz. Therefore, we believe a high-order low-pass filter with a cutoff frequency at 10 Hz can effectively minimize the impact of environmental noise.

Next, we perform amplitude demodulation by multiplying the geophone signal with itself. That is, we treat the geophone signal as its own carrier signal. For our objective of estimating heart rate and respiratory rate, we only need to recover their frequency components, but not phase information. As such, we can simply set both signals' phases to be 0. Then, based on Equation 1, we have

$$
\begin{aligned}
s^2(t) &= (s_r * \sum_{j=1}^{N} s_{h_j})^2 \\
&= a_i' * cos(4\pi f_r t) + \sum_{j=1}^{2N} (a_{h_j}' * cos(2\pi f_{h_j} t)) \\
&\quad + \sum_{j=1}^{2N} (a_{h-_j}' * cos(2\pi (f_{h_j} - 2f_r)t)) \\
&\quad + \sum_{j=1}^{2N} (a_{h+_j}' * cos(2\pi (f_{h_j} + 2f_r)t))
\end{aligned}
\tag{2}
$$

The multiplication result consists of several low frequency components that are less than $1 Hz$ and many frequency components that are greater than or equal to $1 Hz$. As we observe from Equation 2, the lowest frequency component, $a_1 * cos(4\pi f_r t)$, has twice the frequency of the respiration signal. If we can identify this particular component, we can derive the respiration frequency.

Figure 4 shows an example of the demodulation result. After applying a low-pass filter with a cutoff frequency of 0.6 Hz, we successfully remove the high frequency energy. Then, we compute the square root of the filtered signal in time domain and obtain the low frequency signal in frequency domain at 0.253 Hz (about 15.2 BPM_{rr}) which is the respiratory rate.

4 MONITORING TARGET HEART RATE WHEN MULTIPLE SUBJECTS ARE PRESENT

In this section, we discuss how we monitor the heart rate for the target person – say, Alice – when she shares a bed with Bob. In order to achieve this objective, we need to be able to extract Alice's heartbeat signal from the geophone signal in which both heartbeat signals are lumped together. In this study, we aim to separate the two heartbeat signals (their frequency components) so that we can extract either if needed. That way we can monitor the physiological signs for both people on the bed.

4.1 Modeling Mixture Signals

We first formulate the heartbeat separation problem by formally defining the mixed signal [35]. Suppose we have 2 signal sources s_1 and s_2, with signals $s_1(t)$ and $s_2(t)$, respectively. Suppose we have 2 geophone receivers x_1 and x_2, which receive mixed signals $x_1(t)$ and $x_2(t)$ such that

$$x_k(t) = \sum_{j=1}^{2} a_{k,j} s_j(t - \delta_{k,j}), k = 1, 2, \qquad (3)$$

where $a_{k,j}$ and $\delta_{k,j}$ are the attenuation coefficients and time delay parameters associated with the path from s_j to x_k. Since we don't have prior knowledge of the true signal attenuation and delay in our system, we rely on relative signal attenuation and delay. Here, we consider $x_1(t)$ as reference signal (with $a_{1,1} = a_{1,2} = 1$ and $\delta_{1,1} = \delta_{1,2} = 0$), and compare $x_2(t)$ to it to obtain the corresponding relative attenuation and delay coefficients.

After calculating the short-time Fourier transform (STFT) of $x_1(t)$ and $x_2(t)$, we obtain their time-frequency representation:

$$\begin{bmatrix} \hat{x}_1(\tau, \omega) \\ \hat{x}_2(\tau, \omega) \end{bmatrix} = P_{2\times2} \begin{bmatrix} \hat{s}_1(\tau, \omega) \\ \hat{s}_2(\tau, \omega) \end{bmatrix}, \qquad (4)$$

where the propagation matrix $P_{2\times2}$ is defined as

$$P_{2\times2} = \begin{bmatrix} 1 & 1 \\ a_{2,1}e^{-i\omega\delta_{2,1}} & a_{2,2}e^{-i\omega\delta_{2,2}} \end{bmatrix}. \qquad (5)$$

In Figure 5, We illustrate our experiment setting which includes two subjects (s_1 and s_2) and two geophone sensors (x_1 and x_2). The direct propagation paths from s_1 to both geophone sensors are marked in green, and the paths from s_2 to both geophone sensors are marked in brown. Using the same color, we also mark the corresponding attenuation coefficients and time delay parameters.

4.2 Background on Blind Source Separation and the DUET Algorithm

Our heartbeat separation problem is similar to the cocktail party problem [20] where an arbitrary number of people are talking simultaneously at a cocktail party and a listener is trying to identify and follow one particular discussion. DUET [48, 55] has proven to be a good solution to the cocktail party problem. It computes the symmetric attenuation and relative delay of the signals, calculates the energy histogram within different ranges of attenuation-delay values, and finally identifies each energy peak as a signal source.

This is suitable for the cocktail party problem because it cleverly leverages the unique properties of audio signals. Audio signals have spatial signatures as the attenuation and delay parameters between
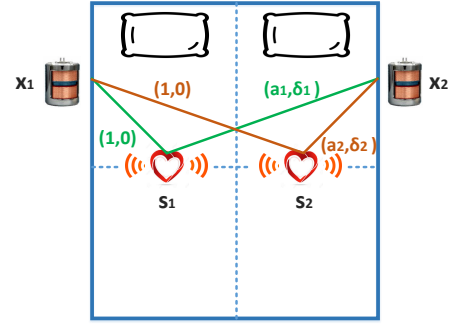

Figure 5: We illustrate our experiment setting, which includes two subjects (s_1 and s_2) and two geophone sensors (x_1 and x_2). We mark the corresponding attenuation coefficients and time delay parameters on the figure, using green for one source and brown for the other source.

an audio source and the receiver are unique. In addition, mixture audio signals usually have sparse frequency components because it is rare to have two people talking at the same frequency at the same time.

In this study, we choose to adopt DUET due to the similarity between audio signals and heartbeat signals. Firstly, both heartbeat signals and audio signals have a fundamental frequency component and high frequency components (harmonics). Secondly, we have no control of, nor a priori knowledge of, the frequencies of heartbeat signals or audio signals. Thirdly, the paths between different sources and receivers have diversity, making it possible to establish spatial features for each source.

Heartbeat signals, however, have their own characteristics. For examples, heartbeat signals have much narrower frequency ranges than audio signals; heartbeats from multiple people have less frequency difference than audio signals; the frequency of heartbeat signals fluctuates from beat to beat while audio signals are consistent for at least a few cycles. These characteristics may not satisfy the implicit assumptions made by DUET and impose challenges in our system design. We will explain how we tackle these challenges in the rest of this section.

4.3 Heartbeat Signal Separation and Heart Rate Estimation

Next, we present our algorithm that separates individual heartbeat signals and estimates each person's heart rate.

Here we assume we have two synchronized geophone receivers that continuously collect mixed signals from two subjects. We partition the signals into processing windows of equal length (40 seconds) and apply the following signal processing steps on both signals within the same window:

(1) *Filtering.* We apply a suitable low-pass filter to filter out environmental noise (discussed in Section 4.3.1), and then remove the direct current (DC) component from the filtered signal;

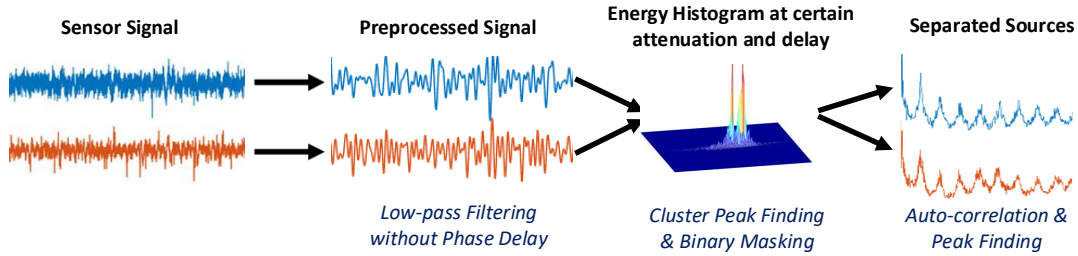(2) *STFT.* We compute the STFT results of the two filtered signals (discussed in Section 4.3.2);

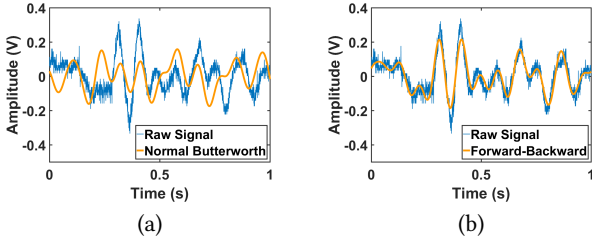**Figure 6: Overview of our heartbeat separation algorithm.**

Figure 7: (a) A normal Butterworth filter introduces phase delays, while (b) a forward-backward filter can leave the filtered signal in perfect alignment with the original signal.
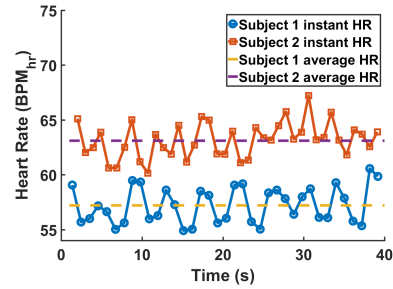

Figure 8: The instantaneous heart rates of two participates at a calm state, fluctuate around their average heart rates, 57.2 and 63.1 BPM_{hr}.

(3) *Spatial Signatures.* We calculate symmetric attenuation and relative delay between the two STFT results (discussed in Section 4.3.3);

(4) *Energy Clustering.* We calculate the energy of each frequency bin (we partition the entire frequency range into discrete bins) and sum the energy values for different ranges of symmetric attenuation and relative delay. We then rebuild the signals in the new coordinate system with the relative delay on x-axis, symmetric attenuation on y-axis and the energy histogram on z-axis (discussed in Section 4.3.3);

(5) *Binary Masking.* We identify the coordinates of the peaks in this new three-dimensional space and apply a binary mask to separate peaks that represent different heartbeats (discussed in Section 4.3.4);

(6) *Heart Rate Estimation.* We convert the signal from the frequency domain back to the time domain, and then estimate the heart rate using the method discussed in [13, 27]. We also estimate the respiratory rate using the algorithm in Section 3.

Figure 6 pictorially shows these steps involved in our algorithm.

4.3.1 FFT and Low-pass Filtering for Noise Reduction. Geophone signals are usually highly noisy because the sensor is quite sensitive, and therefore efficient noise reduction becomes an essential step. We note that, as mentioned in Section 3, most of the noise is above 11 Hz while the target signals are mainly below 15 Hz. Therefore, a high-order Butterworth low-pass filter with cut-off frequency at 10 Hz can effectively reduce the noise.

Since DUET separates signals from different sources using their spatial signatures, we want to make sure the filtering step does

not cause any signal distortions that may change the signal signature. For this purpose, we perform a high-order low-pass Butterworth filter, followed with a forward-backward digital filtering technique [50]. By applying this forward-backward digital filter technique in both directions, the phase distortions caused by the two filters cancel out each other. Eventually, we introduce no phase distortion at all.

Shown in Figure 7(b), the signal after the forward-backward digital filter aligns perfectly with the original signal, while a normal high-order low-pass Butterworth filter introduces delay between the original signal and the resulting signal (Figure 7(a)). In addition, the forward-backward filter also squares the amplitude response. Finally, after applying the low-pass filter, we remove the DC component since it contains no heartbeat related information.

4.3.2 Time-Frequency Representation for Locating Spatial Information. In this step, we obtain the time-frequency representation of the filtered signals. We choose STFT for this purpose.

Lack of Short-Term Frequency Stability: Audio signals usually have stable frequency components within a short time window. Rabiner [47] pointed out that audio signal frequencies within a 45 ms time window can be considered stable. However, this is not true for heartbeats. As shown in Figure 8, the instantaneous heart rate fluctuates considerably around the average heart rate. Hence, compared to the audio signal, the heartbeat signal's frequency varies a lot more from cycle to cycle. As a result, when we compute STFT, we have to further partition the signals within a processing window of 40 seconds into smaller segments.

Insufficient Frequency Difference: For any pair of signals that have the same length, $s_1(t)$ and $s_2(t)$, they are W-disjoint orthogonal when they satisfy:

$$\hat{s}_1(\tau, \omega)\hat{s}_2(\tau, \omega) = 0, \forall \tau, \omega, \tag{6}$$

where $\hat{s}_1(\tau, \omega)$ and $\hat{s}_2(\tau, \omega)$ are the time-frequency representation of signal $s_1(t)$ and $s_2(t)$, respectively. It means that the energy from one source is much larger than the other source.

This assumption doesn't hold true for signals at the same frequency. The sum of any two signals at the same frequency, regardless of their amplitude and phase values, constitutes a single signal at that frequency. As a result, if we don't have additional information about the two signals' amplitude and phase information, we can't separate them since there are an infinite number of ways of decomposing the mixed signal. As such, heartbeat separation does not work if the individual heartbeats are at the same frequency.

Though it is rare for two people to have exactly the same heartbeats, it is quite often that their heartbeat frequencies are close to each other due to the small heartbeat frequency range. For example, let us consider two heartbeat signals whose frequencies are 1 Hz and 1.1 Hz respectively. In order to discriminate the two signals, we actually need at least a 10-second signal to see the difference: one has 10 beats within 10s, while the other one has 11 beats. However, it is very hard, if not impossible, for a heartbeat signal to hold steady at a the same frequency for a duration of 10 seconds.

Our Solution: In VitalMon, we deal with these challenges by the following tricks. First, we focus on the heartbeat signal's high frequency components for more sparsity. For example, for heartbeat signals at 1 Hz and 1.1 Hz, their eighth harmonics – 8 Hz and 8.8 Hz respectively – have greater frequency difference. Second, we partition each processing window (40 seconds) into much smaller slots to ensure the two signals are W-disjoint orthogonal during each slot. Figure 9 plots the heart rate estimation error with different slot durations. Generally, a slot duration less than 1.7 seconds leads to much lower estimation error. In particular, we find the slot duration around 0.7 second yields the lowest estimation error, 1.90 BPM_{hr}. In our evaluation, we then adopt a slot duration of 0.7 second for our heartbeat separation and extraction.

4.3.3 Calculating Symmetric Attenuation and Relative Delay. From the STFT results, we are able to compute the relative attenuation and relative delay as in [55]:

$$\hat{a}(\tau, \omega) = \left| \frac{\hat{x}_2(\tau, \omega)}{\hat{x}_1(\tau, \omega)} \right|, \tag{7}$$

$$\hat{\theta}(\tau, \omega) = -\frac{1}{\omega} \angle \frac{\hat{x}_2(\tau, \omega)}{\hat{x}_1(\tau, \omega)}, \tag{8}$$

where $\hat{x}_1(\tau, \omega)$, $\hat{x}_2(\tau, \omega)$ are the time-frequency representation from the STFT results, and ω is the frequency vector. Considering that symmetric attenuation yields higher resolutions when signals from the same source get different attenuation at different receivers, we further compute the estimated symmetric attenuation:

$$\tilde{\alpha}(\tau, \omega) = \hat{a}(\tau, \omega) - \frac{1}{\hat{a}(\tau, \omega)}. \tag{9}$$

Combining symmetric attenuation and relative delay, we are able to separate signals from the two sources. The next step is to compute the energy histogram based on the attenuation-delay
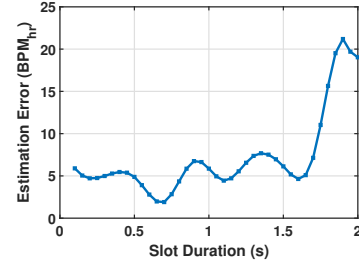

Figure 9: The mean absolute estimation error (in BPM_{hr}) with different slot durations. The slot duration of 0.7 second gives the best estimation, with an error of 1.90 BPM_{hr}.

values. For any given frequency that falls into the range that has the same symmetric attenuation and relative delay, we compute the energy histogram by summing up the estimated energy in those frequency ranges. Following this process, we eventually cluster the frequencies that are from the same source and have similar symmetric attenuation and relative delay values.

4.3.4 Finding Cluster Peaks and Applying Binary Masking in 3D Space. Next, we explain how we find cluster peaks, which each correspond to a separate signal. In our problem, symmetric attenuation and delay values from different sources overlap with each other, leading to poorly formed clusters that are hard to identify. As a result, we cannot rely on normal peak finding algorithms or machine learning algorithms such as K-Means Clustering [33], or CLIQUE [11] to identify the peaks.

Instead, we take advantage of the spatial diversity in our system. If we place geophone x_2 close to Alice, and x_1 close to Bob, and use $x_1(t)$ as the reference, then symmetric attenuation of Alice's heartbeat signal is positive while symmetric attenuation of Bob's heartbeat signal is negative. Then, we can use a simple binary mask to assign each attenuation-delay pair to either Alice or Bob.

4.3.5 Estimating Target Heart Rate. Once signals from different sources are properly separated, we perform inverse STFT to return them to the time domain. We then apply the heartbeat detection algorithm discussed in [27] to extract the heartbeats. Namely, we compute the signal power, calculate the sample auto-correlation function (ACF), find peaks in the sample ACF results [7], and finally convert the peak locations to corresponding heartbeat pulses. Once we obtain the heart rates, we associate each heart rate to the correct person on the bed, based on the location information. Meanwhile, we also apply our respiratory rate estimation algorithm in Section 3.2 on each heartbeat signal to estimate each subject's breathing rate.

5 VITALMON TESTBED

Amplifier and ADC: In our testbed, we use two SM-24 geophones [4] to track the heart rate and respiratory rate. The raw analog signal from each geophone is first amplified through its own amplifier circuit whose amplification is 200. Then, the amplified signals are fed into a 12-bit analog-to-digital converter (ADC) on an Arduino Due [1] whose range is 0 to 3.3 V and sampling frequency is 2.5 kHz. Meanwhile, the two geophone signals are synced through the internal clock of the Arduino Due. Figure 10 shows the experiment
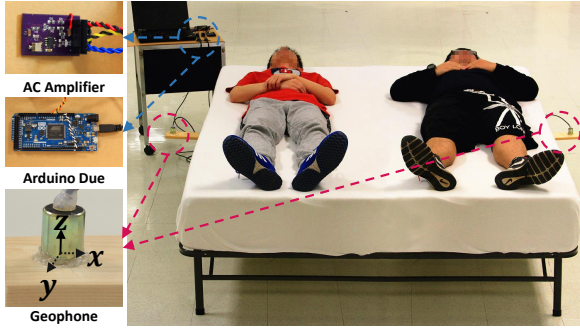
Figure 10: Our prototype bed. We install two geophone boards that are sandwiched between the mattress and the frame, one on each side of the bed.

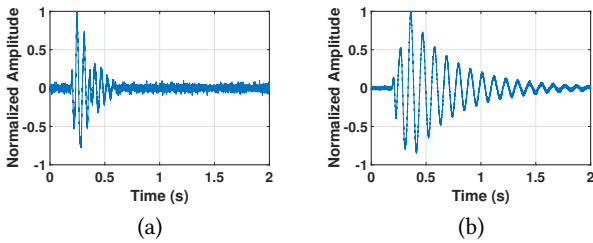(a)   (b)

Figure 11: When we gently tap the prototype bed, response from a vertical geophone (a) is much more crisp (shorter oscillation) than the response from a horizontal geophone (b).

setting with two participants on our prototype bed. The bed has a memory foam mattress and a steel frame.

Vertical vs Horizontal Geophones: Many geophones respond to vibrations in a single direction, although more complex geophones that can sense vibrations in multiple directions are available. In our experiments, we have tried vertical geophones (responding to vibrations in the z direction in Figure 10) and horizontal geophones (responding to vibrations in the $x - y$ plane in Figure 10). Through experimentation, we choose vertical geophones in our testbed. We explain the reason below.

Our first intuition was to choose horizontal geophones. Each heartbeat is mainly caused by the sudden ejection of blood during the ventricle systole. The direction of such momentary ejection first goes from the ventricle to the aorta and then gets split to different blood vessels of a human body. Due to such directionality, the strongest vibration is along the head-foot direction (in the $x - y$ plane). Intuitively, we would like to capture the strongest vibration by using multiple horizontal geophones.

However, when we consider the human body, the bed, the floor and our system as a whole piece, we find horizontal geophones a poor choice because beds are designed to allow the joints to be underdamped on the $x - y$ plane, yielding more horizontal oscillations. Such oscillations usually last for more than 1 second, which is one heartbeat cycle, such that a heartbeat may last long enough to affect the following heartbeat(s). On the other hand, we find vertical geophones experience much smaller and shorter oscillations because oscillations in the z direction are damped against the floor.As a result, horizontal geophones and multi-dimension
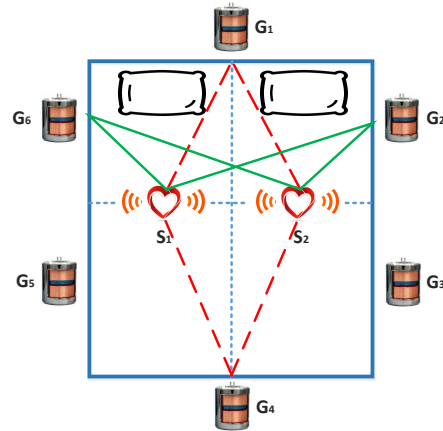

Figure 12: This figure shows the top view of a bed, that has two sources s_1 and s_2. Here we show two example installation plans. The plan marked by red dashed lines represents a poor installation where two sources have same symmetric attenuation and relative delay. The plan marked by green solid lines is a good installation.

geophones that can measure horizontal vibrations are not suitable for our system.

Figures 11 (a) and (b) show the responses from a vertical geophone and a horizontal geophone when we lightly tap the bed just once. For each signal, we normalized the amplitude to observe how long the oscillation lasts. The tapping motion occurred at time 0.2 second. The vertical oscillation lasted for roughly 0.3 second, while the horizontal oscillation lasted for more than 1.8 seconds.

Geophone Placement: Next, we carefully consider how the two geophones should be placed on the bed. Our heartbeat separation algorithm involves inferring the symmetric attenuation and relative delay information from the amplitude and phase of frequencies in the signal STFT. To avoid any ambiguity of phase delay caused by phase wrap [14], we should not separate the two geophone sensors by more than half of the wavelength of the signal. Fortunately, in our case, this requirement is easy to satisfy because the wavelength of the heartbeat signal is usually much larger than the length of a regular bed. For example, for a heartbeat signal whose rate is 60 bpm, its wavelength roughly is 1 km.

Our technique separates signals from different sources by their unique spatial signatures. As a result, when we install geophone sensors, we need to make sure there is difference between the sources' spatial signatures. Suppose the two hearts' positions are s_1 and s_2, and the two geophones' positions are x_1 and x_2. Then we need to the following inequality is satisfied

$$\frac{||x_1 s_1||}{||x_1 s_2||} \neq \frac{||x_2 s_1||}{||x_2 s_2||},$$

where $||x_1 s_1||$ is the distance between x_1 and s_1. In Figure 12, we illustrate six possible geophone positions named G_1, ..., and G_6 in the clockwise sequence and the two heartbeat locations. In this example, we cannot place the following geophone pairs, (G_1, G_4), (G_2, G_3), and (G_5, G_6). Any of the rest of the combinations could
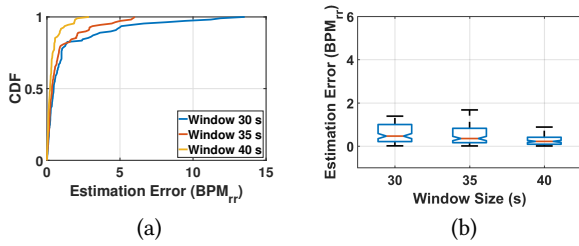
(a)   (b)

Figure 13: CDF (a) and box plot (b) of the respiratory rate estimation error when we have a single subject, with the processing window of 30, 35, and 40 seconds. Window length of 40 seconds has the best results – mean estimation error of 0.38 BPM_{rr}, and median error of 0.22 BPM_{rr}, over 525 samples – which is then adopted in the rest of the evaluation.

work well for our purpose. In our testbed, we mount the two geophones according to $(G6, G2)$ in the diagram.

6 EVALUATION

In this section, we use our testbed to evaluate VitalMon in the following aspects: (1) estimating the respiratory rate for a single subject, (2) estimating the target subject's heart rate when two subjects are present, and (3) estimating the target subject's respiratory rate when two subjects are present. Also, we have a discussion on the real world deployment.

6.1 Monitoring a Single Subject's Respiratory Rate

We conducted 525 experiments and recorded more than 350 minutes data from a total of 23 subjects. We report the respiratory rate estimation error as the absolute difference between the estimated BPM_{rr} and the ground truth $\overline{BPM}_{rr}$.

Participants: We had a total of 23 healthy volunteer participants for this experiment, including 14 males and 9 females. The mean age of the participants was 25.14 years with a standard deviation of 3.42 years. The youngest participant was 21 years old while the oldest was 34 years old.

During each experiment, subjects were asked to lie on the prototype bed and breathe at a certain rate for the duration of 40 seconds. Specifically, we played a metronome at 1 tick per second and asked the subjects to breathe in and out every 2, 3, 4, 5, or 6 ticks (the respiratory rate during each experiment was thus fixed). We manually monitored the participant's breathing rate by observing how his/her chest moved during the experiment. Each subject went through at least 20 experiments and in total we conducted 525 experiments.

Figures 13(a) and (b) show the cumulative distribution function (CDF) and a box plot of the estimation error with different processing window lengths. Both plots show that larger window sizes yield lower estimation errors: we have mean error of 0.38 BPM_{rr}, and median error of 0.22 BPM_{rr}, when the window length is 40 seconds. In the rest of the evaluation, we use the processing window of 40 seconds. We also note that a median estimation error of 0.22 BPM_{rr} and a mean estimation error of 0.38 BPM_{rr} are better than many other systems when estimating the breathing rate for a single

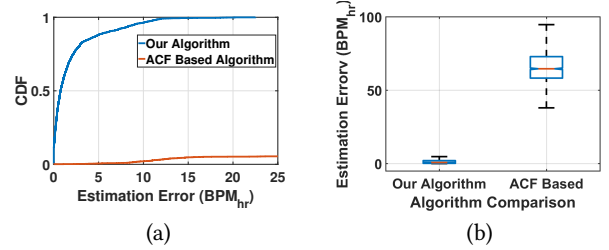(a)   (b)

Figure 14: We compare the heart rate estimation error of our algorithm with the ACF-based heartbeat separation algorithm: (a) CDF, and (b) box plot of the estimation error. Our algorithm yields much lower estimation error.

subject. For example, the estimation error reported in [13, 21] is 0.47 and above 2 BPM_{rr}, respectively.

6.2 Monitoring Target Heart Rate when Multiple Subjects are Available

In this part of the evaluation, we conduct more than 3000 experiments and record more than 33 hours of geophone data from a total of 35 subjects. We compare the estimated BPM_{hr} against the ground truth $\overline{BPM}_{hr}$ measured by a medical grade pulse oximeter [6] and report the estimation error.

Participants: We had a total of 35 healthy volunteer participants for this experiment, including 19 males and 16 females. The mean age of the participants was 25.26 years with a standard deviation of 3.25 years. The youngest participant was 21 years old while the oldest was 35 years old.

6.2.1 Mean Heart Rate Estimation Error. We first conducted a series of experiments to evaluate how our algorithm performs over a large range of heart rates while two subjects share the prototype bed (without gross body motions). To ensure we evaluate our system over a large range of heart rates, we asked one of the two subjects to exercise (e.g. running outdoor, climbing stairs, etc.) for a few minutes before each experiment. The participants lay on their back in this set of experiments.

We collected 952 experiments in this part, including a large range of heart rates that range from 43 to 137 BPM_{hr}. Figure 15 shows the estimation error over different heart rate ranges. Based on the ground truth heart rate collected by a pulse oximeter, we group the 4304 samples (we have two samples per experiment) into 6 groups: < 60, $[60, 70)$, $[70, 80)$, $[80, 90)$, $[90, 100)$, and ≥ 100. The median and the mean of overall estimation error over more than 4000 samples is 0.72 and 1.90 BPM_{hr}, respectively. We note that this result, which evaluates two subjects together, is in the range of other systems that detect a single person's heart rate (e.g., mean error of 1.17 BPM_{hr} in [13] and mean error around 2 BPM_{hr} in [32]).

Comparison with the ACF-based Approach: We next compare our algorithm with the direct ACF-based heartbeat detection algorithm (results shown in Figure 14), where we use our ACF-based heart rate estimation algorithm, but don't first separate the signal. Instead, we assume geophone x_1's signal is dominated by $s_1(t)$, and use the ACF-based heartbeat detection algorithm in [27] to directly count the heartbeats in $x_1(t)$ for s_1. Similarly, we run the same algorithm on $x_2(t)$ to count heartbeats for s_2. We show that our
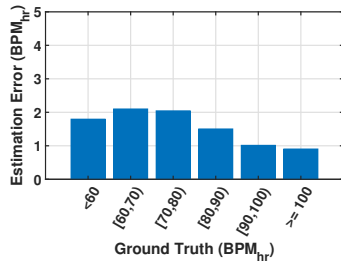
Figure 15: When two subjects share a bed, average heart rate estimation errors are shown for each of the following heartbeat rate ranges: < 60, $[60, 70)$, $[70, 80)$, $[80, 90)$, $[90, 100)$, ≥ 100. Over more than 1900 samples, our mean error is 1.90 BPM_{hr}, and median error is 0.72 BPM_{hr}.
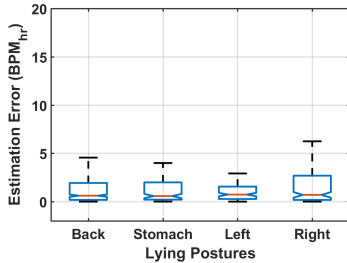

Figure 16: The box plot of the heart rate estimation error when two subjects share a bed and lie in different postures, including lying on back/stomach/left/right. Our mean estimation error is below 2.5 BPM_{hr} and median error is below 0.74 BPM_{hr} regardless of the posture, suggesting our system is robust against different lying postures.

algorithm has a much lower estimation error, mean error of 1.90 BPM_{hr}, compared to the ACF based algorithm whose mean error is 66.53 BPM_{hr}. The ACF-based separation approach works poorly because it often captures both heartbeats from each geophone signal.

6.2.2 The Impact of Lying Posture. In this part, we conducted 1203 experiments to evaluate the impact of lying posture on our performance. During each experiment, two subjects were asked to adopt one of the following postures: (1) lying on back, (2) lying on stomach, (3) lying on his/her left side, and (4) lying on his/her right side. The length of each experiment is again 40 seconds.

Figure 16 shows the box plot of the heart rate estimation error for different lying postures. The results show that our system is robust against different lying postures – the mean estimation error for lying on back, stomach, left, and right is 1.75, 1.62, 2.17, and 2.47 BPM_{hr}, respectively, while the median error is 0.61, 0.57, 0.73, and 0.70 BPM_{hr}. We note that the estimation error when the subject was lying on the right is slightly higher because the heart position is slightly further away from the mattress in this posture.

6.2.3 The Impact of Different Mattress Type. We also conducted 901 experiments to evaluate the impact of different mattress types, including a memory foam mattress (our default mattress), a spring mattress, and a hardwood mattress. Figure 17 shows that the mean estimation error for these three types of mattresses is 1.85, 2.44,
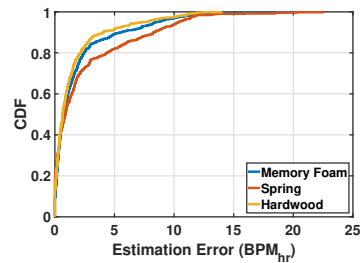

Figure 17: CDF of the heart rate estimation error when two subjects share a bed with different mattress types. A spring mattress has slightly higher estimation error than a hardwood or a memory foam mattress.

and 1.53 BPM_{hr}, respectively, while the median error is 0.73, 0.88, and 0.66 BPM_{hr}. The results are as expected – among these three mattress types, a hardwood one adds to the least oscillations to the geophone signal while a spring mattress has the most oscillation. However, we argue that even with the spring mattress which gives the highest estimation error, the estimation accuracy is still sufficient for most applications.

6.3 Monitoring Target Respiratory Rate When Multiple Subjects are Present

In this part of the evaluation, we conducted 1503 experiments on our prototype bed and recorded more than 16 hours of data. During each experiment, we didn't give any instructions on how the subjects should breathe. We evaluate the performance of our respiration detection algorithm by comparing the estimated respiratory rate against the ground truth measured by a Zephyr bioharness belt [8] and report the estimation error.

Participants: We had a total of 28 healthy volunteer participants for this experiment, including 15 males and 13 females. The mean age of the participants was 24.79 years with a standard deviation of 2.99 years. The youngest participant was 21 years old while the oldest was 34 years old.

Experiment Procedure: We conducted more than 1500 experiments and evaluated our algorithm over a large range of respiratory rates, from 8.61 to 25.09 BPM_{rr}. Before experiments, some subjects were asked to exercise, including running, climbing stairs, etc.

Based on the respiratory rate measured by a Zephyr belt, we grouped the 3006 samples into 5 groups: <12, $[12, 15)$, $[15, 18)$, $[18, 21)$, and ≥ 21 BPM_{rr}. Figure 18 shows that the overall mean estimation error across more than 3000 samples is 2.62 BPM_{rr}, while the median error is 1.95 BPM_{rr}. We note that this result is worse than our single-person breathing rate estimation because we have to go through two levels of indirection in estimate breathing rate when multiple people share a bed. In our on-going work, we are developing techniques to improve our performance in this case.

Next, we evaluate how different types of sleep postures affect our estimation error. Figure 19 shows that lying postures have little impact on estimating respiratory rate – the average estimation error for these different postures (lying on back/stomach/left/right) is 2.77, 2.36, 2.68, and 2.40 BPM_{rr}, respectively while the median error is 2.15, 1.66, 2.09, and 1.67 BPM_{rr}.
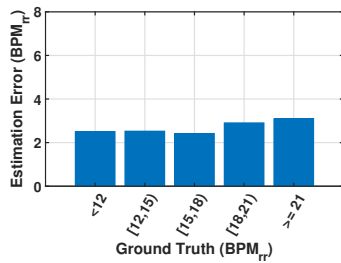
Figure 18: When two subjects share a bed, mean breathing rate estimation errors are shown for each of the following breathing rate ranges: < 12, $[12, 15)$, $[15, 18)$, $[18, 21)$, ≥ 21 – 2.51, 2.53, 2.42, 2.90, 3.09 BPM_{rr}, respectively. The average error rate across all the 2406 samples is 2.62 BPM_{rr}, while the median error is 1.95 BPM_{rr}.
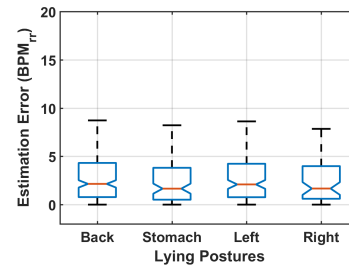

Figure 19: Box plot of the breathing rate estimation error when two subjects share a bed and lie in different postures, including lying on back/stomach/left/right. The average estimation errors for these different postures are very close to each other.

6.4 Discussion on Real World Deployment

Real world deployment of our system could potentially enable quite a few interesting applications. So far, we have shown our system can monitor heart rate and respiratory rate for one or two people on a bed. We have found our system is also able to detect a user's gross body motions, or smaller activities such as snores during sleep. These functions combined , we could build a more sophisticated sleep monitoring system that can accurately detect a person's sleep stage and evaluate the sleep quality. To achieve this objective, we need to carefully tune several system parameters to detect and classify these fine-grained information. One possible solution is to add more geophone sensors at different locations to form a small-scale sensor network that facilitates more accurate separation of various target signals.

7 RELATED WORK

In this section, we categorize different vital sign monitoring systems in two ways: (1) systems which detect the heart rate and respiratory rate of a single person, e.g. [13, 16–19, 24, 27, 30, 32, 40, 52]; (2) systems which detect heart rate and respiratory rate of two people simultaneously, such as the system shown in [10, 32]. Also, we summarize their signal processing methods for heart rate and respiratory rate estimation.

7.1 Vital Sign Monitoring of a Single Person

There are diverse systems proposed to detect heartbeats and respiration of a single person. So far, it is the most commonly studied field.

Sensors installed under the thorax area: Bu et al. [19] inserted a piezoelectric sensor which measures the pressure fluctuation due to heartbeats and respiration. The detected signal is processed by Empirical Mode Decomposition and the vital sign signals are reconstructed by summing up the signal within the predefined frequency range. Bruser et al. [18] packaged a Wheatstone bridge of four sensitive load cells onto one slat from the slatted frame and measured the vibration caused by heartbeats. An unsupervised learning technique is used to extract the shape of a single heart beat from the signal. In [17], an array of photodetectors under the mattress are used to detect the change of reflected and scattered light caused by vibration. The heartbeat and respiration signals can be separated by applying a simple low-order high-pass filter. Šprager et al. [52] used an optical sensor which transmitted and received interferometric signal to capture optical variation caused by vibrations from heartbeat and respiration. Later a wavelet-based decomposition technique was applied to extract heartbeats and respiration signal from the received signal. Kortelainen et al. [30] deployed several pressure sensitive foils under the mattress. The heartbeats were extracted from the channel averaged cepstrum based on Fourier transformation, while respiration is calculated by an adaptive principal component analysis. Aubert et al. [13] put a foil pressure sensor in the thorax area under a thin mattress to detect vital signs during sleep. The heart rate and respiratory rate are obtained from analyzing the autocorrelation function after applying appropriate bandpass filters.

Sensors that requires special cushion: Heise et al. [24] deployed four hydraulic-transducer tubes under the mattress and showed three possible signal processing strategies (a Window-based Peak-to-Peak Deviation algorithm, a K-means clustering algorithm, and a Hilbert transform algorithm) to extract the heartbeats. Yamana [54] designed an ultrasound transmitter and receiver system mounted under a plywood support. The system is placed under the mattress and measures the shape change of the plywood support. A simple bandpass filter is applied to separate the heartbeat signal.

Sensors installed under the bed post: Nukaya et al. [40] proposed to use a piezoceramic system to detect heartbeats. Four sensors were bonded to two metal plates on top and bottom, then sandwiched between floor and bed posts. A simple bandpass filter was applied to get the heartbeat signal. Brink et al. [16] built a set of four optical load cells which were installed under each bed post and directly find the heartbeats as the local maximums after low-pass filtration.

Wearable Sensors: Phan et al. [45] uses a chest belt with a built-in biaxial accelerometer to measure the vibrations on the surface of the chest cavity. A bandpass filter is applied to extract the respiration signal, and a combination of envelope detection and peak finding algorithm is used for estimating the heart rate.

Mobile Sensors: Nandakumar et al. [37] detects sleep apnea events within a meter by turning a smartphone into a sonar system. The

system emits frequency-modulated sound signals and detects the frequency shifts of the reflections due to chest movements.

Sensors that can be attached to anywhere on the bed frame: Jia et al. [27] proposed a heartbeat monitoring system based on an on-the-shelf geophone which could be inserted anywhere between a mattress and a bed frame. A combination of low-pass filter, sample auto-correlation function and peak finding algorithm are used to extract the periodicity of heartbeats. An evaluation of real world data varying different types of bed and house environment shows the possibility of using the system in daily heartbeat monitoring.

7.2 Vital Sign Monitoring of Multiple People

Only a few papers addressed detecting multiple people's vital signs simultaneously. Adib et al. [10] use a wireless radar to measure the distance change of a human chest, due to heartbeats and respiration. The device can send Frequency Modulated Carrier Waves (FMCW) which can isolate signals from different distances, and then estimate the heart rate and respiratory rate of multiple people via FFT. Liu et al. [32] use WiFi to measure the Channel State Information (CSI) of the reflections off the human body. The system takes the advantages of Received Signal Strength (RSS) from multiple subcarriers and estimates the heart rate and respiratory rate by using a power spectral density based algorithm. RSS values are sensitive to the multipath situation in the environment, and therefore wireless systems that are based on RSS readings may be affected by the changes in the environment.

8 CONCLUDING REMARKS AND FUTURE DIRECTION

In this paper, we discuss and evaluate an unobtrusive, vibration-based vital sign monitoring system during sleep. Our system centers around a geophone sensor that can sense the vibration velocity caused by ballistic force. Compared to earlier geophone-based in-bed vital sign monitoring systems that could only detect heartbeats from a subject lying in bed, our system is significantly improved. First, it can monitor the subject's breathing rate, even though geophones cannot directly detect breathing. Second, it can track the subject's heart rate and breathing rate when he/she shares the bed with another person. In this case, vibrations caused by multiple heartbeats are mixed together and need to be separated. After involving 86 participants and collecting 56 hours of geophone data, we show that our system is accurate and can work in different scenarios (e.g., lying postures, mattress types).

Going forward, there are several important directions we plan to investigate, including (1) obtaining better signal-to-noise ratio for more accurate heart rate and respiratory rate monitoring; (2) understanding the physical respiration phenomenon better and adjusting our respiration model accordingly; (3) investigating the time and frequency characteristics of gross body motions and updating our model accordingly.

ACKNOWLEDGMENT

REFERENCES

[1] Arduino due. https://www.arduino.cc/en/Main/arduinoBoardDue.
[2] Fitbit. https://www.fitbit.com/.
[3] Gearfit2. http://www.samsung.com/global/galaxy/gear-fit2/.
[4] Geophone sm-24. https://www.sparkfun.com/products/11744.
[5] Murata contactless bed sensor. http://www.murata.com/en-us/products/sensor/accel/sca10h_11h.
[6] Neulog heart rate & pulse logger sensor. https://neulog.com/heart-rate-pulse/.
[7] Peak finding and measurement. http://terpconnect.umd.edu/~toh/spectrum/PeakFindingandMeasurement.htm.
[8] Zephyr performance systems. https://www.zephyranywhere.com/benefits/physiological-biomechanical.
[9] *Analog Communication(Jntu)*. McGraw-Hill Education (India) Pvt Limited, 2006.
[10] F. Adib, H. Mao, Z. Kabelac, D. Katabi, and R. C. Miller. Smart homes that monitor breathing and heart rate. In *Proceedings of the 33rd Annual ACM Conference on Human Factors in Computing Systems*, pages 837–846. ACM, 2015.
[11] R. Agrawal, J. Gehrke, D. Gunopulos, and P. Raghavan. *Automatic subspace clustering of high dimensional data for data mining applications*, volume 27. ACM, 1998.
[12] M. Apps, P. Sheaff, D. Ingram, C. Kennard, and D. Empey. Respiration and sleep in parkinson's disease. *Journal of Neurology, Neurosurgery & Psychiatry*, 48(12):1240–1245, 1985.
[13] X. L. Aubert and A. Brauers. Estimation of vital signs in bed from a single unobtrusive mechanical sensor: Algorithms and real-life evaluation. In *Engineering in Medicine and Biology Society, 2008. EMBS 2008. 30th Annual International Conference of the IEEE*, pages 4744–4747. IEEE, 2008.
[14] J. M. Blackledge. *Digital signal processing: mathematical and computational methods, software development and applications*. Elsevier, 2006.
[15] J. Box and G. M. Jenkins. *Reinsel. Time Series Analysis, Forecasting and Control*. Prentice Hall, Englewood Cliffs, NJ, USA, 3rd edition edition, 1994.
[16] M. Brink, C. H. Müller, and C. Schierz. Contact-free measurement of heart rate, respiration rate, and body movements during sleep. *Behavior research methods*, 38(3):511–521, 2006.
[17] C. Bruser, A. Kerekes, S. Winter, and S. Leonhardt. Multi-channel optical sensor-array for measuring ballistocardiograms and respiratory activity in bed. In *Engineering in Medicine and Biology Society (EMBC), 2012 Annual International Conference of the IEEE*, pages 5042–5045. IEEE, 2012.
[18] C. Bruser, K. Stadlthanner, S. de Waele, and S. Leonhardt. Adaptive beat-to-beat heart rate estimation in ballistocardiograms. *Information Technology in Biomedicine, IEEE Transactions on*, 15(5):778–786, 2011.
[19] N. Bu, N. Ueno, and O. Fukuda. Monitoring of respiration and heartbeat during sleep using a flexible piezoelectric film sensor and empirical mode decomposition. In *Engineering in Medicine and Biology Society, 2007. EMBS 2007. 29th Annual International Conference of the IEEE*, pages 1362–1366. IEEE, 2007.
[20] E. C. Cherry. Some experiments on the recognition of speech, with one and with two ears. *The Journal of the acoustical society of America*, 25(5):975–979, 1953.
[21] B. Fang, N. D. Lane, M. Zhang, A. Boran, and F. Kawsar. Bodyscan: Enabling radio-based sensing on wearable devices for contactless activity and vital sign monitoring. In *Proceedings of the 14th Annual International Conference on Mobile Systems, Applications, and Services*, pages 97–110. ACM, 2016.
[22] R. Fletcher and J. Han. Low-cost differential front-end for doppler radar vital sign monitoring. In *Microwave Symposium Digest, 2009. MTT'09. IEEE MTT-S International*, pages 1325–1328. IEEE, 2009.
[23] J. Gordon. Certain molar movements of the human body produced by the circulation of the blood. *Journal of Anatomy and Physiology*, 11(Pt 3):533, 1877.
[24] D. Heise, L. Rosales, M. Sheahen, B.-Y. Su, and M. Skubic. Non-invasive measurement of heartbeat with a hydraulic bed sensor progress, challenges, and opportunities. In *2013 IEEE International Instrumentation and Measurement Technology Conference (I2MTC)*, pages 397–402. IEEE, 2013.
[25] D. Heise, L. Rosales, M. Skubic, and M. J. Devaney. Refinement and evaluation of a hydraulic bed sensor. In *Engineering in Medicine and Biology Society, EMBC, 2011 Annual International Conference of the IEEE*, pages 4356–4360. IEEE, 2011.
[26] A. Hyvärinen, J. Karhunen, and E. Oja. *Independent component analysis*, volume 46. John Wiley & Sons, 2004.
[27] Z. Jia, M. Alaziz, X. Chi, R. E. Howard, Y. Zhang, P. Zhang, W. Trappe, A. Sivasubramaniam, and N. An. Hb-phone: A bed-mounted geophone-based heartbeat

monitoring system. In *2016 15th ACM/IEEE International Conference on Information Processing in Sensor Networks (IPSN)*, pages 1–12. IEEE, 2016.

[28] I. Jolliffe. *Principal component analysis*. Wiley Online Library, 2002.

[29] R. E. Kleiger, J. P. Miller, J. T. Bigger, and A. J. Moss. Decreased heart rate variability and its association with increased mortality after acute myocardial infarction. *The American journal of cardiology*, 59(4):256–262, 1987.

[30] J. M. Kortelainen, M. van Gils, and J. Parkka. Multichannel bed pressure sensor for sleep monitoring. *Computing in Cardiology*, 39:313–316, 2012.

[31] C. Langton. Hilbert transform, analytic signal, and the complex envelope. *Signal Processing and Simulation Newsletter*, 1999.

[32] J. Liu, Y. Wang, Y. Chen, J. Yang, X. Chen, and J. Cheng. Tracking vital signs during sleep leveraging off-the-shelf wifi. In *Proceedings of the 16th ACM International Symposium on Mobile Ad Hoc Networking and Computing*, pages 267–276. ACM, 2015.

[33] S. Lloyd. Least squares quantization in pcm. *IEEE transactions on information theory*, 28(2):129–137, 1982.

[34] D. C. Mack, J. T. Patrie, P. M. Suratt, R. A. Felder, and M. Alwan. Development and preliminary validation of heart rate and breathing rate detection using a passive, ballistocardiography-based sleep monitoring system. *Information Technology in Biomedicine, IEEE Transactions on*, 13(1):111–120, 2009.

[35] R. Mersereau and T. Seay. Multiple access frequency hopping patterns with low ambiguity. *IEEE Transactions on Aerospace and Electronic Systems*, pages 571–578, 1981.

[36] M. Mirshekari, S. Pan, P. Zhang, and H. Y. Noh. Characterizing wave propagation to improve indoor step-level person localization using floor vibration. In *SPIE Smart Structures and Materials+ Nondestructive Evaluation and Health Monitoring*, pages 980305–980305. International Society for Optics and Photonics, 2016.

[37] R. Nandakumar, S. Gollakota, and N. Watson. Contactless sleep apnea detection on smartphones. In *Proceedings of the 13th Annual International Conference on Mobile Systems, Applications, and Services*, pages 45–57. ACM, 2015.

[38] K. Narkiewicz, N. Montano, C. Cogliati, P. J. Van De Borne, M. E. Dyken, and V. K. Somers. Altered cardiovascular variability in obstructive sleep apnea. *Circulation*, 98(11):1071–1077, 1998.

[39] J. Nolan, P. D. Batin, R. Andrews, S. J. Lindsay, P. Brooksby, M. Mullen, W. Baig, A. D. Flapan, A. Cowley, R. J. Prescott, et al. Prospective study of heart rate variability and mortality in chronic heart failure. *Circulation*, 98(15):1510–1516, 1998.

[40] S. Nukaya, T. Shino, Y. Kurihara, K. Watanabe, and H. Tanaka. Noninvasive bed sensing of human biosignals via piezoceramic devices sandwiched between the floor and bed. *Sensors Journal, IEEE*, 12(3):431–438, 2012.

[41] S. Pan, A. Bonde, J. Jing, L. Zhang, P. Zhang, and H. Y. Noh. Boes: building occupancy estimation system using sparse ambient vibration monitoring. In *SPIE Smart Structures and Materials+ Nondestructive Evaluation and Health Monitoring*, pages 90611O–90611O. International Society for Optics and Photonics, 2014.

[42] S. Pan, C. G. Ramirez, M. Mirshekari, J. Fagert, A. J. Chung, C. C. Hu, J. P. Shen, H. Y. Noh, and P. Zhang. Surfacevibe: vibration-based tap & swipe tracking on ubiquitous surfaces. In *IPSN*, pages 197–208, 2017.

[43] T. Park. *Introduction to Digital Signal Processing: Computer Musically Speaking*. World Scientific, 2010.

[44] D. O. Pederson and K. Mayaram. Demodulators and detectors. *Analog Integrated Circuits for Communication*, pages 457–484, 2008.

[45] D. Phan, S. Bonnet, R. Guillemaud, E. Castelli, and N. P. Thi. Estimation of respiratory waveform and heart rate using an accelerometer. In *Engineering in Medicine and Biology Society, 2008. EMBS 2008. 30th Annual International Conference of the IEEE*, pages 4916–4919. IEEE, 2008.

[46] J. G. Proakis. Digital communications. *McGraw-Hill, New York*, 1995.

[47] L. R. Rabiner. A tutorial on hidden markov models and selected applications in speech recognition. *Proceedings of the IEEE*, 77(2):257–286, 1989.

[48] S. Rickard. The duet blind source separation algorithm. *Blind Speech Separation*, pages 217–237, 2007.

[49] L. Rosales, M. Skubic, D. Heise, M. J. Devaney, and M. Schaumburg. Heartbeat detection from a hydraulic bed sensor using a clustering approach. In *Engineering in Medicine and Biology Society (EMBC), 2012 Annual International Conference of the IEEE*, pages 2383–2387. IEEE, 2012.

[50] J. O. Smith. *Introduction to digital filters: with audio applications*, volume 2. Julius Smith, 2008.

[51] S. Šprager and D. Zazula. Heartbeat and respiration detection from optical interferometric signals by using a multimethod approach. *IEEE transactions on biomedical engineering*, 59(10):2922–2929, 2012.

[52] S. Šprager and D. Zazula. Detection of heartbeat and respiration from optical interferometric signal by using wavelet transform. *Computer methods and programs in biomedicine*, 111(1):41–51, 2013.

[53] T. Watanabe and K. Watanabe. Noncontact method for sleep stage estimation. *IEEE Transactions on biomedical engineering*, 51(10):1735–1748, 2004.

[54] Y. Yamana, S. Tsukamoto, K. Mukai, H. Maki, H. Ogawa, and Y. Yonezawa. A sensor for monitoring pulse rate, respiration rhythm, and body movement in bed. In *Engineering in Medicine and Biology Society, EMBC, 2011 Annual International Conference of the IEEE*, pages 5323–5326. IEEE, 2011.

[55] O. Yilmaz and S. Rickard. Blind separation of speech mixtures via time-frequency masking. *IEEE Transactions on signal processing*, 52(7):1830–1847, 2004.